

Perceptual quality evaluation of some anti line-flicker filters

Citation for published version (APA):

Boschman, M. C., & Martens, J. B. (1996). *Perceptual quality evaluation of some anti line-flicker filters*. (IPO-Rapport; Vol. 1131). Instituut voor Perceptie Onderzoek (IPO).

Document status and date:

Published: 29/10/1996

Document Version:

Publisher's PDF, also known as Version of Record (includes final page, issue and volume numbers)

Please check the document version of this publication:

- A submitted manuscript is the version of the article upon submission and before peer-review. There can be important differences between the submitted version and the official published version of record. People interested in the research are advised to contact the author for the final version of the publication, or visit the DOI to the publisher's website.
- The final author version and the galley proof are versions of the publication after peer review.
- The final published version features the final layout of the paper including the volume, issue and page numbers.

[Link to publication](#)

General rights

Copyright and moral rights for the publications made accessible in the public portal are retained by the authors and/or other copyright owners and it is a condition of accessing publications that users recognise and abide by the legal requirements associated with these rights.

- Users may download and print one copy of any publication from the public portal for the purpose of private study or research.
- You may not further distribute the material or use it for any profit-making activity or commercial gain
- You may freely distribute the URL identifying the publication in the public portal.

If the publication is distributed under the terms of Article 25fa of the Dutch Copyright Act, indicated by the "Taverne" license above, please follow below link for the End User Agreement:

www.tue.nl/taverne

Take down policy

If you believe that this document breaches copyright please contact us at:

openaccess@tue.nl

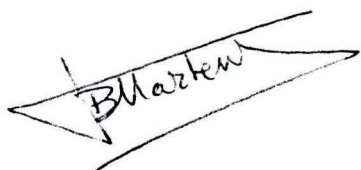
providing details and we will investigate your claim.

Rapport no. 1131

Perceptual quality evaluation of
some anti line-flicker filters

M.C. Boschman and J.B. Martens

Voor akkoord: Dr.ir. J.B. Martens



J.B. Martens

Contents

1. Introduction	1
2. Temporal artifacts of TV sets	1
2.1 Field-flicker	1
2.2 Line-flicker	1
2.3 Phi-movement	2
3. Adaptive flicker-reduction filtering	2
4. Experiments	2
4.1 Subjective quality evaluation	2
4.2 Apparatus and procedure	3
4.3 Experiment 1: Optimization of adaptive filters	4
4.4 Experiment 2: Quality evaluation of fixed and adaptive filters	9
5. General conclusions	15
References	15
Appendix: Adaptive flicker-reduction filtering	i

Perceptual quality evaluation of some anti line-flicker filters

Martin Boschman and Jean-Bernard Martens

Institute for Perception Research (IPO)

P.O. Box 513, 5600 MB Eindhoven, The Netherlands

Email: boschman@natlab.research.philips.com

jbm@natlab.research.philips.com

1. Introduction

This report describes the results of a study at the request of Philips Media Systems (PMS). A product that PMS has in mind is a converter that enables TV viewers to watch VGA pictures that are produced by their personal computer. Their motive is the rising popularity of surfing the internet with pages that typically contain text, graphical information and photographic pictures. When text and graphical information is displayed on a 50 Hz interlaced TV-set in most cases line-flicker will become an unacceptably annoying artefact. Adequate spatial low-pass filtering along the vertical direction may reduce line-flicker while keeping the overall quality at an acceptable level. A negative side-effect of spatial filters is the introduction of unsharpness which may have an effect on the legibility of text and on the overall perceptual image quality. A trade-off between the presence of line-flicker and spatial unsharpness is evident. This makes it a typical optimization problem.

Adaptive filters are expected to be useful as they only become active at positions where line-flicker is likely to occur. The aim of this study was to develop some adaptive low-pass filters and evaluate them together with some fixed low-pass filters on their effectiveness to reduce line-flicker while maintaining overall image quality.

2. Temporal artifacts of TV sets

Below three visual disturbance phenomena that may appear on a 50 Hz interlaced TV-system are briefly described.

2.1 Field-flicker

Field-flicker on a TV-set is a global attribute caused by temporal modulation by vertical blanking. The field-flicker frequency equals the field repetition rate i.e. 50 Hz. Spatial filtering has no effect on field flicker. Therefore, this artifact will not be considered in this study.

2.2 Line-flicker

Line-flicker is a temporal artifact of the interlace principle. When displaying an image in 50 Hz 2:1 interlaced mode, the image is divided in two fields containing the odd and even lines respectively. Both fields are displayed with a temporal resolution of 25 Hz, but are interlaced in time, which causes an apparent repetition rate of 50 Hz. Any spatial modu-

lation of the luminance of lines with respect to both its neighbours (low-high-low or high-low-high) will cause a 25 Hz temporal component for which humans are quite sensitive. The effect is integrated over some area so that line-flicker is hardly present in most natural images. In images with horizontal line structures - like text and graphics - line-flicker is quite annoying. Spatial low-pass filtering along the vertical direction will reduce modulation between successive lines and will therefore result in a reduction of line-flicker.

2.3 Phi-movement

Another phenomenon that is present with the interlaced TV system is phi-movement. It is a visual disturbance which is often confused with line-flicker. It is caused by the spatio-temporal modulation between two successive lines which introduces apparent motion. It typically appears at horizontal edges. In the extreme case two successive lines appear as a single line 'dancing' up and down with a frequency of 50 Hz. Low-pass filtering along the vertical direction will also reduce phi-movement.

3. Adaptive flicker-reduction filtering

A general framework for adaptive filtering is described in the Appendix, and this framework is applied to an algorithm for adaptive line-flicker reduction. The algorithm basically distinguishes two steps. First, a line-flicker criterion is derived from the input image. Second, based on this criterion an output image is constructed that is a weighted average of the original image and a low-passed version (along the vertical direction) of this image. In regions where line flicker is expected the low-pass image dominates, while in the remaining regions the original image dominates. We refer to the Appendix for a mathematical description of the algorithm.

4. Experiments

We performed two experiments to evaluate the filters. In the first experiment with 3 participating subjects an optimal set of parameters was obtained for the adaptive filters. In the second experiment 24 subjects evaluated the optimal adaptive filters with window size 2, 3 and 4 together with fixed filters with filter size 2, 3 and 7.

4.1 Subjective quality evaluation

The method we applied is based on a two-alternative-forced-choice paradigm in a paired comparison experiment (Guilford, 1954). For each pair of conditions subjects are asked to indicate which of two conditions (stimuli) they prefer with respect to the overall image quality. After repeatedly presenting all possible combinations we obtain a frequency matrix, indicating how often stimuli are preferred with respect to the other stimuli. From these frequency data the perceived quality was calculated assuming a model according to Thurstone's 'law of comparative judgement' (Thurstone, 1927). The basic assumption of this model is that the strength of the stimulus attribute (in this case perceived image quality) is measured on a psychometric interval scale. Due to internal noise this strength is stochastic with a Gaussian distribution. Estimates of the perceived quality values were obtained in two ways. For the individual (per subject) results we obtained rough estimates

by calculating the average z-score directly from the cumulative proportions (Torgerson, 1958). The pooled results were obtained with the program DIFSCAL (Boschman, 1996) that calculates maximum likelihood estimates for each assessment parameter.

4.2 Apparatus and procedure

Two identical TV-sets (type 21SL5756/00B) were used in the experiment. They were equipped with a standard 50 Hz, 2:1 interlaced scanning system. ‘Contrast’ and ‘Brightness’ of both sets were adjusted so that they had nearly identical luminance transfer characteristics (See Fig 1). Both sets were driven by the RGBS video outputs of two independent CODECs of a DVS ISP-500 display system. The TV-sets were placed next to each other on a table 1.20 m in front of the subjects’ viewing position. This viewing distance is a compromise between the recommended viewing distance of 6 times the height of the active display area ($= 6 \times 0.30 = 1.80$ m) (ITU, 1996) and the distance required for optimal reading of the smallest letters (about 0.90 m) (ISO, 1992). Both sets were placed at a small angle in order to obtain a perpendicular view at both displays (see Fig 2). In order to create living-room-alike conditions the room was illuminated with a few dimmed spot-lights resulting in a background luminance of about $5 \text{ cd} \cdot \text{m}^{-2}$. The subjects were seated at a chair

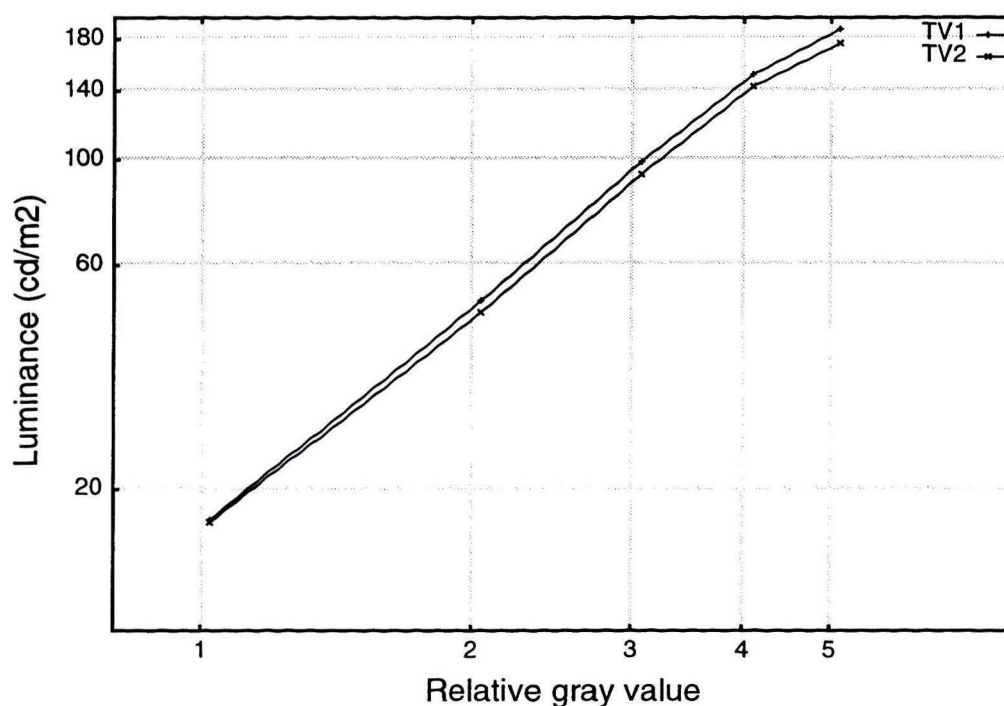


Figure 1: Luminance transfer characteristics measured on a gray bar test pattern for both TV-sets used in the experiments.

behind a small table at which a keyboard and a press-button case were placed. The keyboard was used by the subjects to enter their response ‘1’ or ‘2’ indicating whether they preferred the left or the right condition. The press-button was used to switch between TV-sets while viewing pairs of conditions. This was done in order to prevent crosstalk of visual disturbances between the two displays. Pressing the button caused the right set to be

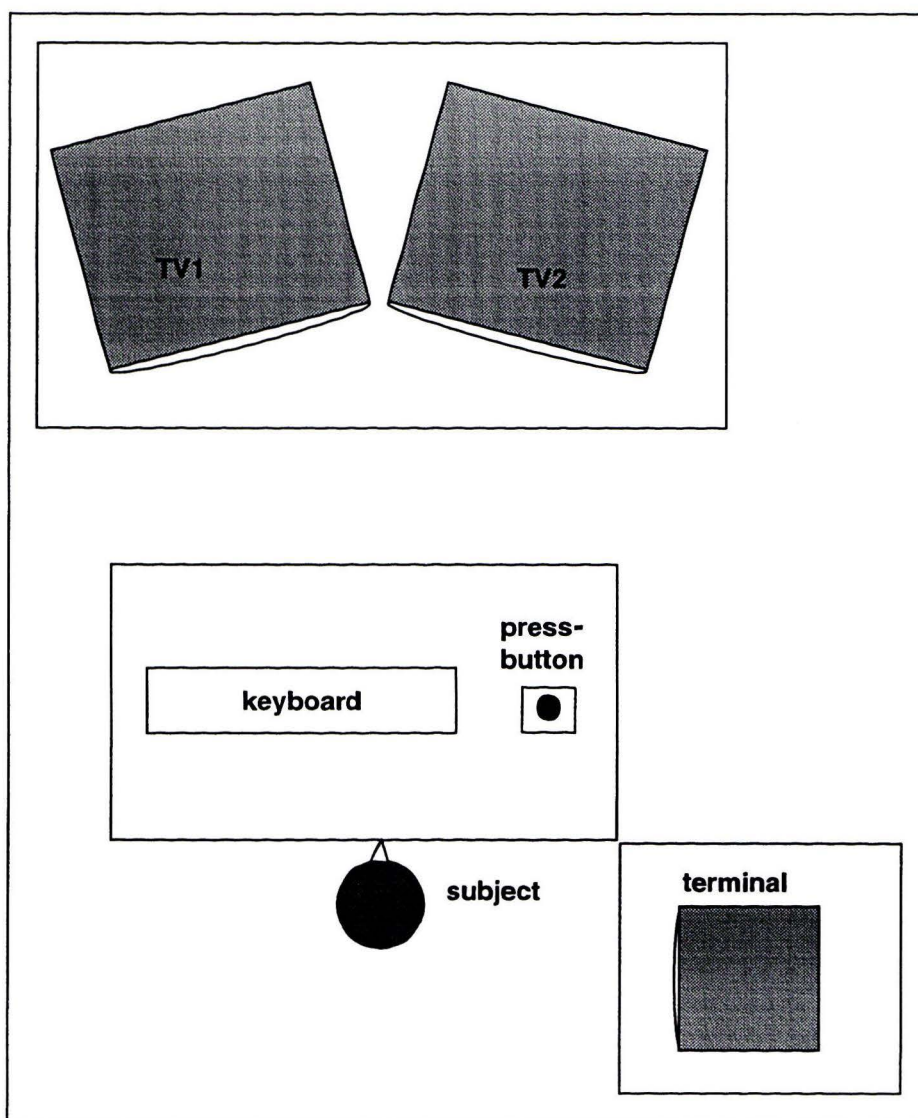


Figure 2: Schematic top view of the configuration of apparatus for the experiments described in the text.

come visible and the left one blanked, while releasing it switched off the right display and made the left one active. The stimulus-pair sequence number was displayed on a terminal on the right of the subject (just out of direct field of view when they watched the TV-sets). Before the experiment the subjects were asked to read the instruction listed in Figure 3. Then a training sequence of 10 pairs was started in order to get acquainted with the task and with the differences between the conditions. The results of this session were not used in the data analysis. The main sequence started immediately after the trial.

4.3 Experiment 1: Optimization of adaptive filters

In the first experiment we were aiming at optimization of the parameters of the adaptive filter. The experiment was divided into 3 independent sessions, each considering one window size (i.e. binomial windows of length 2, 3 and 4). For each window size the length d

Perceptual quality of anti-LF processed TV images

Dear subject,

You are participating in an experiment which is performed in behalf of the VGA-TV project of Philips Media Systems. In this experiment TV-images are processed in various ways with the purpose of reducing annoying line-flicker. A side-effect of this image-processing is a slight appearance of unsharpness. It is important for us to know which processing technique results into optimal image quality with reduced line-flicker and an acceptable level of unsharpness.

In a few minutes a sequence of 120 pairs of images will be presented on the TV-sets in front of you. For each pair of images you are asked to indicate which you prefer with respect to image quality. Before we start the actual experiment, first 10 pairs of images will be presented in order to get used to the task and to give you an impression of the differences that occur among the set of conditions.

At the time the images become available you may use the blue button to display either the left or the right condition. We ask you to compare both images by quickly watching the left and the right TV-set alternately by repeatedly pressing and releasing the blue button. After a short time (about 10 s) both images disappear and will be replaced by a gray field on both sets. Then your task is to indicate which of the two images you prefer with respect to image quality: the left (1) or the right (2) image.

N.B. While making up your quality judgement you are asked to consider both flicker (visual disturbances) and unsharpness. You are also supposed to take the legibility of text (if present) into account.

Please use the keyboard for your response: type '1' or '2' to indicate the display you prefer, and then press ENTER to confirm your answer. If you want to correct your answer, this is only possible before you pressed the ENTER key. The terminal on your right-hand- side will notify you if you entered an invalid answer. If so, you will have the opportunity to enter the answer you had in mind. A new pair of images become available after entering a valid response. On the terminal you will be notified of your progress. After completion of the task the message "Thank you for your time" will appear on the terminal.

Thank you for your cooperation

Martin Boschman

Figure 3: The instruction which was handed to the subject before the experiment. The original instruction was printed in Dutch.

of the line detector filter, the detection threshold parameter t and the slope parameter s were varied as listed in Tables 1 and 2. The adaptivity (line detection and weighing) was calculated for the Y band of the input image and was used to control the low-pass kernel that was applied to the RGB bands of the image. In this experiment we used the image NS1 (see Fig 7) that was captured from a workstation displaying an internet page via Netscape. This image was considered to be rather critical with respect to line flicker and legibility as it contains horizontal line segments and text fragments with small size font.

In the first two sessions the 12 parameter settings of Table 1 were evaluated for binomial windows of size 2 and 4. Three subjects participated in these sessions, all having normal or corrected to normal visual acuity. They performed the two-alternative-forced-choice task as described above. In order to prevent bias effects which might be present due to small differences between the TV-sets, each of the 66 (12x1 1/2) pairs was presented twice in balanced order (e.g. pair AB: first A on set 1, B on set 2 then B on set 1, A on set 2). These sessions lasted about 45 minutes. The pooled results that were analysed with DIFSCAL are plotted in Figures 4 and 5. These results show that in both cases the opti-

Table 1: conditions of the first 2 sessions of experiments 1, considering window size 2 (kernel: 0.5 0.5) and 4 (kernel: 0.125, 0.375, 0.375, 0.125).

	d	t	s
1	1	5	0.1
2	1	5	10
3	1	50	0.1
4	1	50	10
5	3	5	0.1
6	3	5	10
7	3	50	0.1
8	3	50	10
9	5	5	0.1
10	5	5	10
11	5	50	0.1
12	5	50	10

Table 2: conditions of the third session of experiment 1, considering window size 3 (kernel: 0.25, 0.5, 0.25).

	d	t	s
1	3	5	0.1
2	3	5	10
3	3	50	0.1
4	3	50	10

imum length of the line detector filter is $d=3$. Therefore, this length was considered in the third session where the parameters of the adaptive filter with intermediate window size 3 (Table 2) were optimized. In this short (15 minutes) session one of the three subjects evaluated each of the 6 ($=4 \times 3/2$) pairs of conditions six times in balanced order. The results for window size 3 are shown in Figure 6. Since the quality scales are constructed from three independent sessions and are defined up to any linear transformation Figures 4, 5 and 6 are not comparable in absolute sense. However, the results are useful for optimization of the parameters for each window size.

In conclusion, for the applied combinations of parameter settings optimal values were found for d , t and s . For each filter size the optimal detector size is $d = 3$ and the optimal threshold value is $t = 5$. The optimal slope is $s = 10$ for window size 2 and $s = 0.1$ for the filters with window size 3 and 4 (see also Table 3).

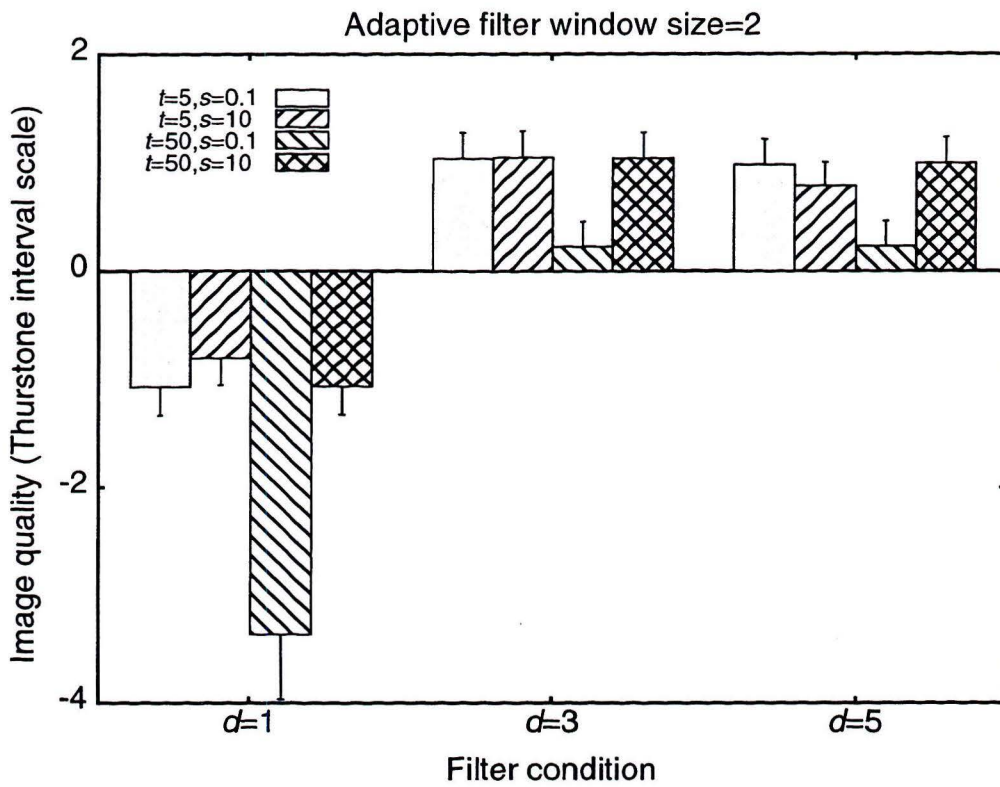


Figure 4: Quality assessment results of experiment 1 for the adaptive filter with binomial window size 2 obtained after analysis of frequency data with DIFSCAL. Each bar corresponds with a combination of settings for the parameters d , t and s . The length of the error bars indicate the standard error of the means.

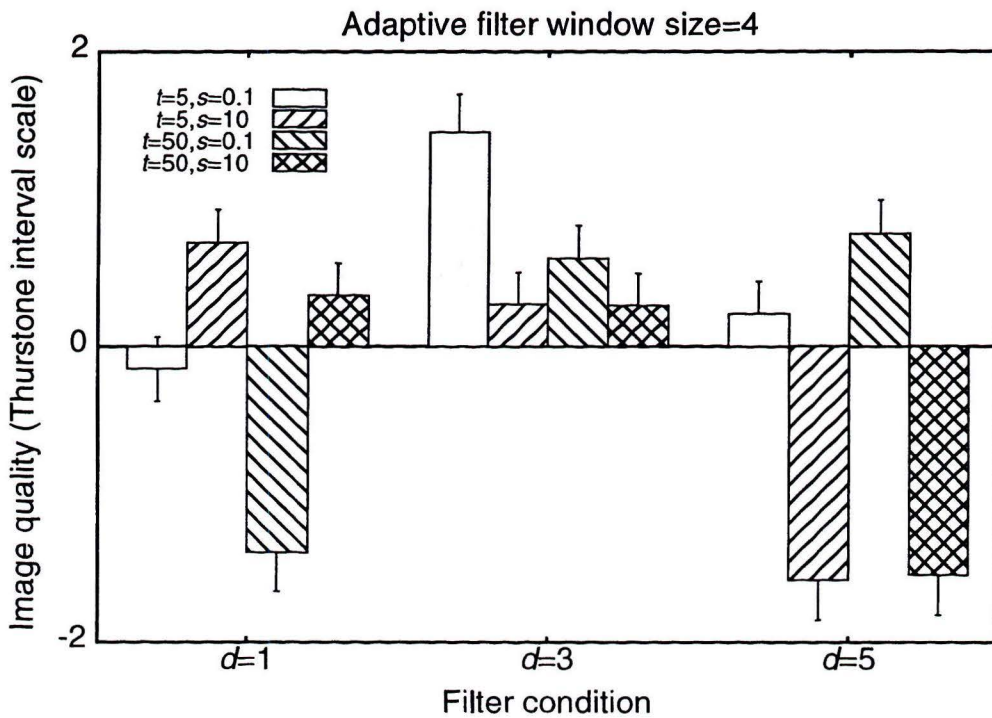


Figure 5: Quality assessment results for the adaptive filter with binomial window size 4.

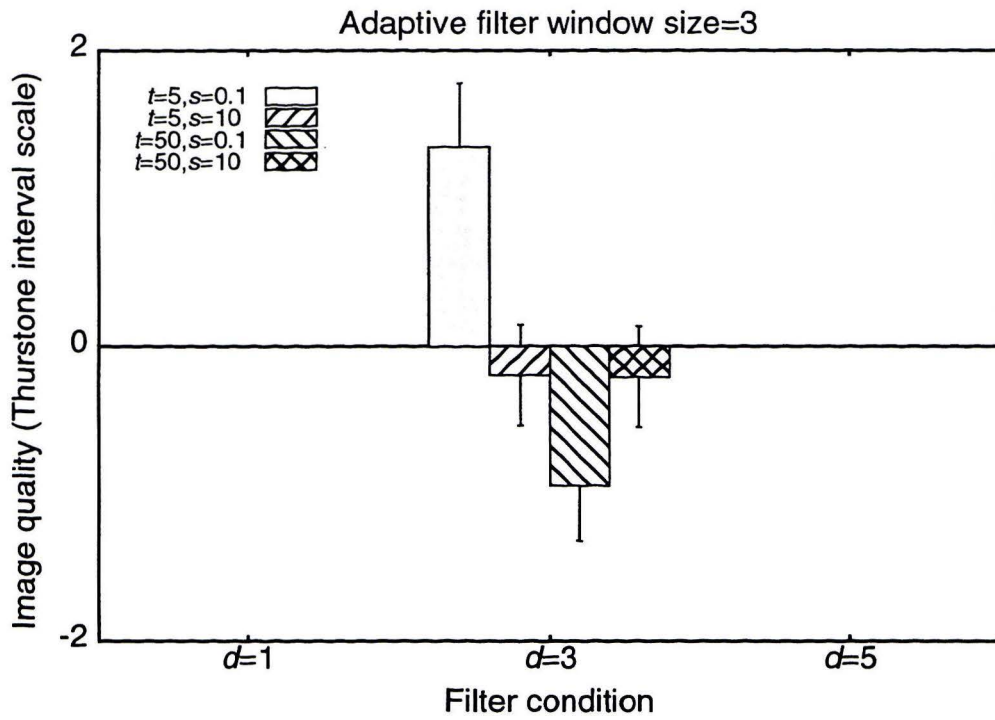


Figure 6: Quality assessment results for the adaptive filter with binomial window size 3.

4.4 Experiment 2: Quality evaluation of fixed and adaptive filters

In this experiment both fixed (filter size 2, 3 and 7) and adaptive (binomial window size 2, 3 and 4) anti line-flicker filters were evaluated. Table 3 shows the characteristics of each applied filter. The adaptive filters are a subset of the filters that were found to be optimal in Experiment 1. All filters kernels did have binomial coefficients, except for the fixed filter with size 7 which contained two negative coefficients causing some deblurring action. The 6 filters were applied to the RGB bands of 4 different images depicted in Figure 7. Three of them (NS1, NS25 and R3) were captured from a workstation displaying an internet page via the Netscape browser. The fourth picture (K29) was a portrait taken from a Kodak photo-CD.

Table 3: Characteristics of the six anti-LF filters that were evaluated in experiment 2. The parameters d , t and s are only relevant for the adaptive filters. The labels are used in Figures 8 and 9.

label	type	size	filter kernel coefficients	d	t	s
f2	fixed	2	0.5 0.5	-	-	-
f3	fixed	3	0.25 0.5 0.25	-	-	-
f7	fixed	7	-0.1133 0.0 0.3438 0.5391 0.3438 0.0 -0.1133	-	-	-
a2	adaptive	2	0.5 0.5	3	5	10
a3	adaptive	3	0.25 0.5 0.25	3	5	0.1
a4	adaptive	4	0.125 0.375 0.375 0.125	3	5	0.1

24 Subjects participated in this experiment, all having normal or corrected to normal visual acuity at the applied viewing distance. After a training session of 10 stimulus pairs they performed the two-alternative-forced-choice task containing a sequence of (4 images) \times (6 \times 5/2 pairs of filter conditions) \times (2 repetitions)=120 stimulus pairs. Again the repetitions were counter-balanced to prevent bias in the results. The total session lasted about 40 minutes per subject.

The results of this experiment are plotted in Figures 8 and 9. Figure 8 depicts the individual scaling results per subject. They were obtained by calculating the average z-score (normal deviate) from the 'preferred' proportions of each condition. The individual data in Figure 8 demonstrate that in most cases subjects do not differ much in their judgement. The DIFSCAL results calculated from the pooled frequency data are plotted in Figure 9. This figure shows that the results for the three Netscape images are highly correlated. In all three cases the fixed filters do score better than the adaptive filters. For these images the fixed filter with size 3 is found to be the best and it scores slightly better than the fixed seven-taps filter. The results for the portrait are different. The effects are smaller than the effects for the Netscape images. The highest quality for this image is obtained with the seven-taps fixed filter.

Obviously the adaptive filters do not sufficiently prevent visual disturbance artifacts. This can only be explained by the property of the detector part of the filter which is designed to indicate positions where line modulation is present. Hence, it only considers line-flicker and not phi-movement. The adaptive filter only activates the low-pass filter

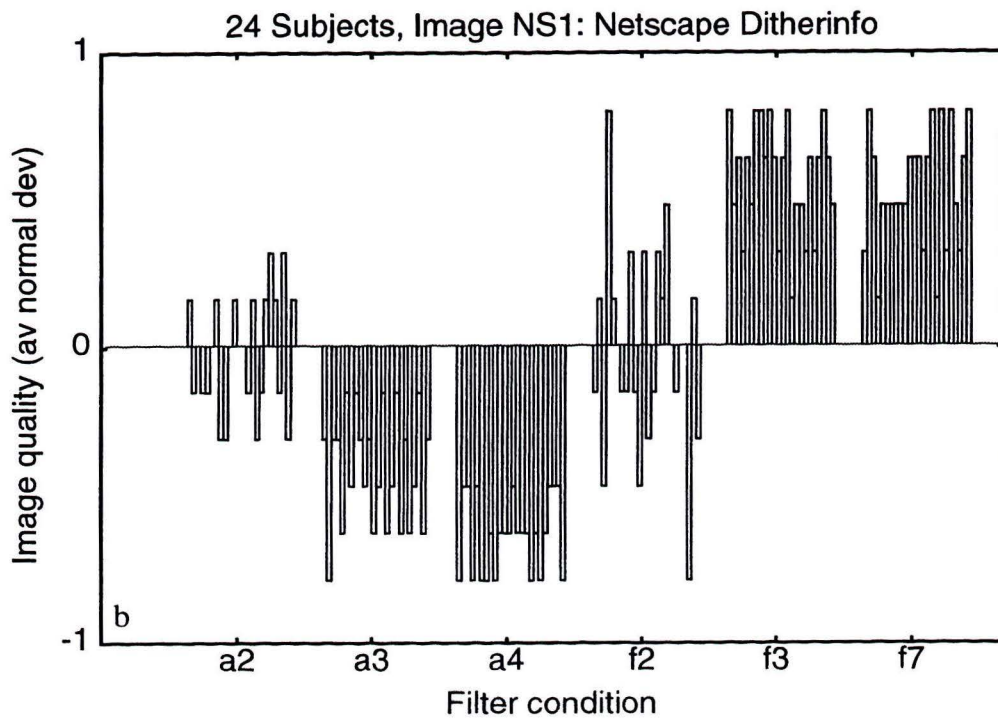
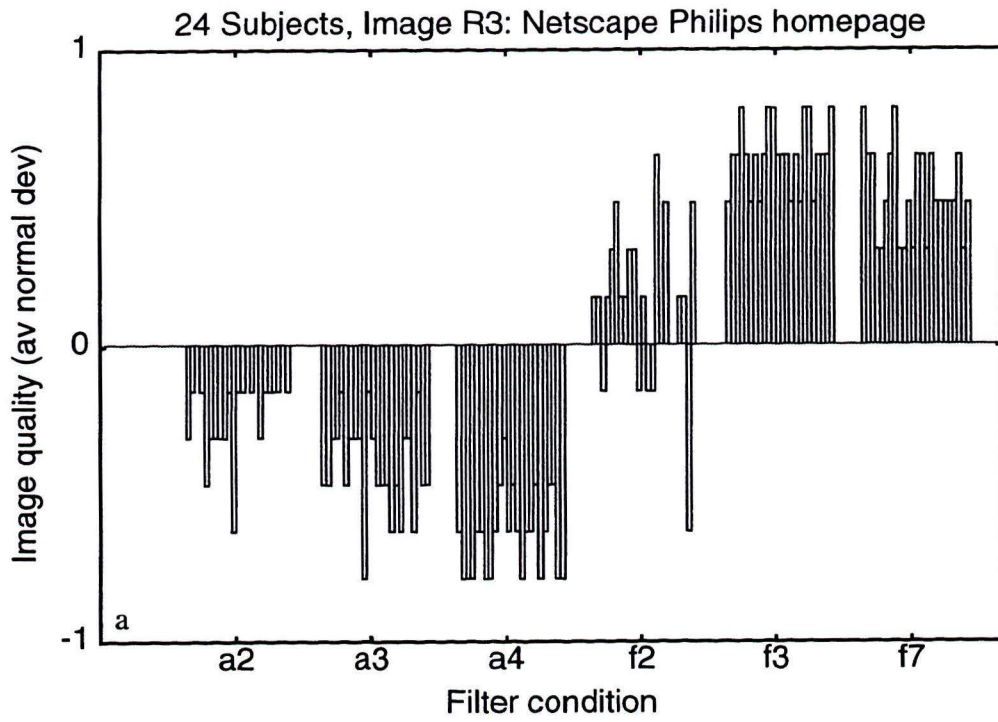


Figure 8a and 8b: Individual results of experiment 2. Each bar corresponds with one subject. The quality value is obtained by averaging the normal deviates for the 'preferred' proportions of that condition. Fig 8a and 8b correspond with the images R3 and NS1.

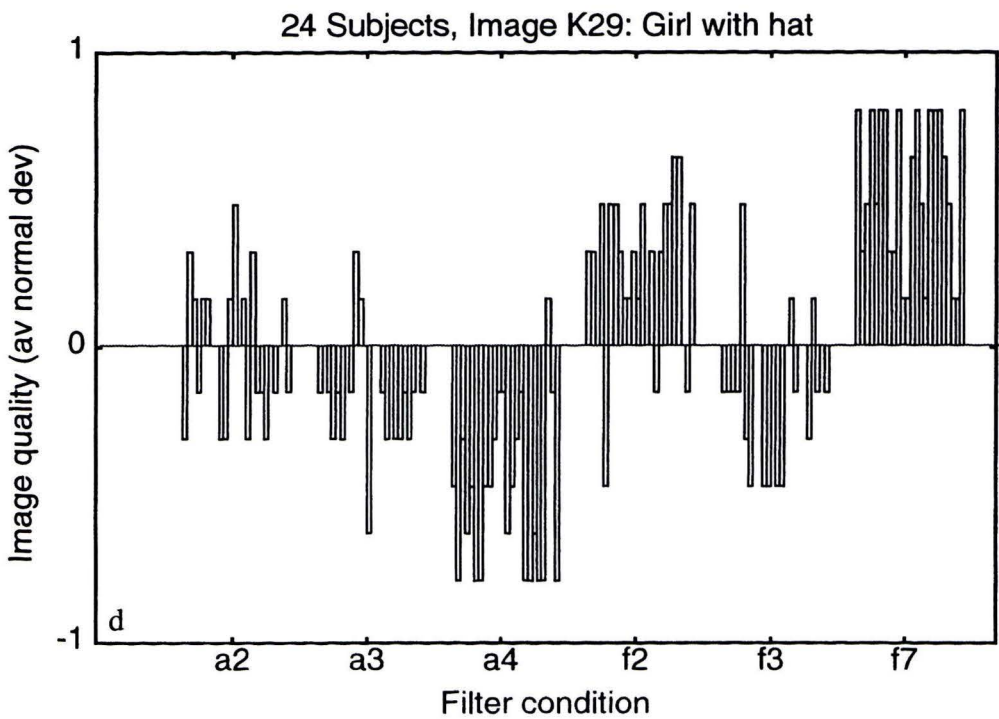
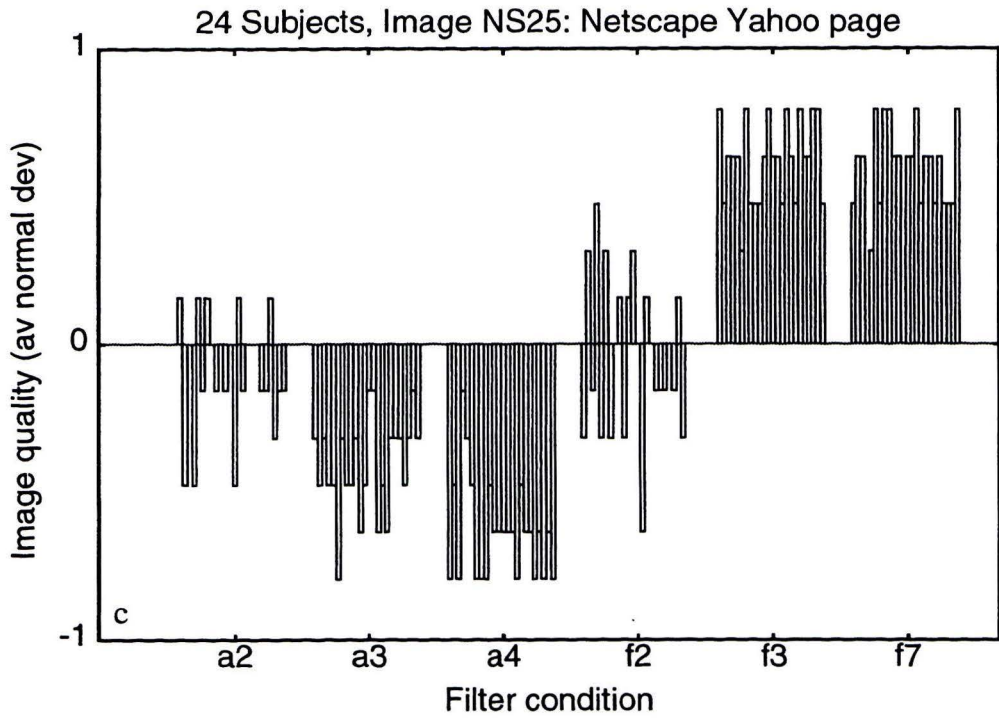


Figure 8c and 8d: The individual results of experiment 2 for images NS25 and K29.

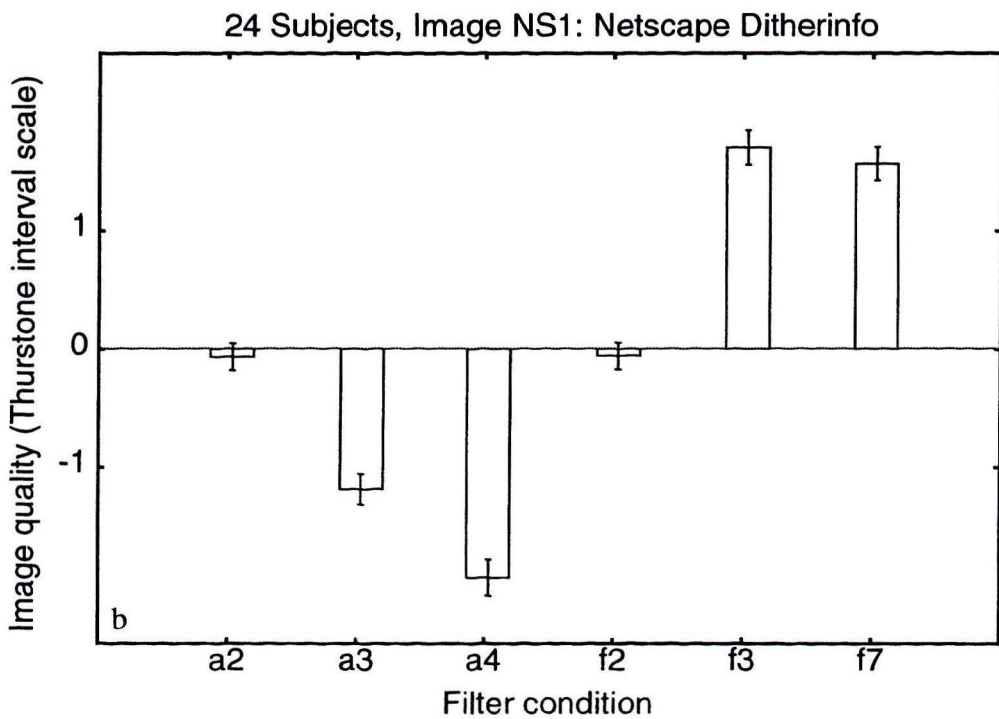
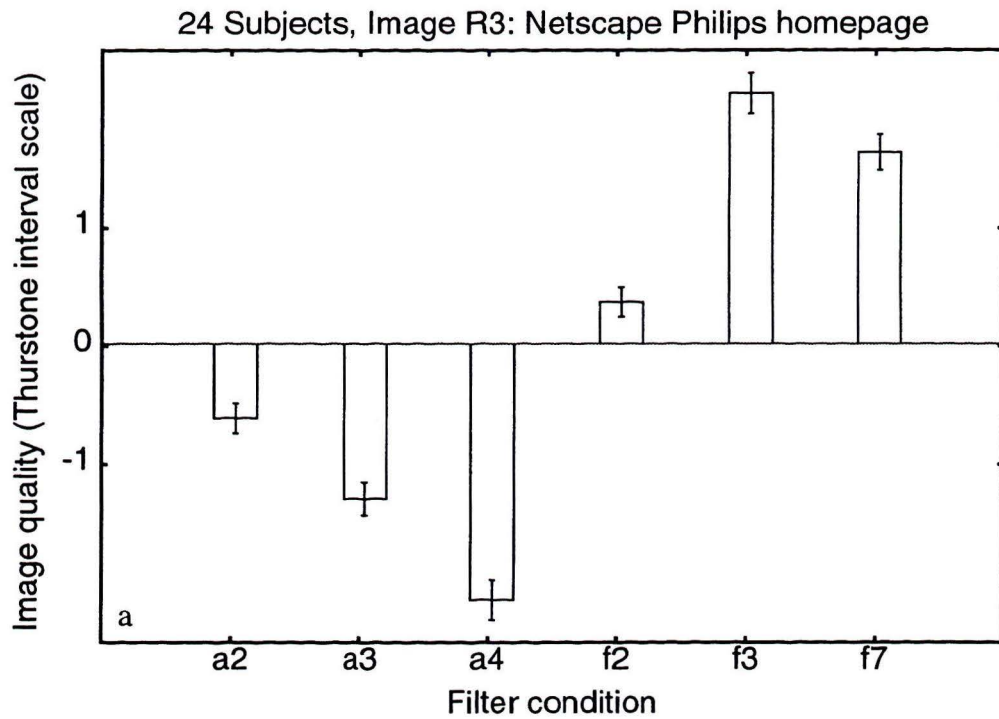


Figure 9a and 9b: Pooled quality assessment results of experiment 2 for images R3 and NS1. The scale values are obtained after analysis of frequency data with DIFSCAL. Each bar corresponds with one filter condition (adaptive: a2, a3 and a4; fixed: f2, f3 and f7). The length of the error bars indicates the standard error of the means.

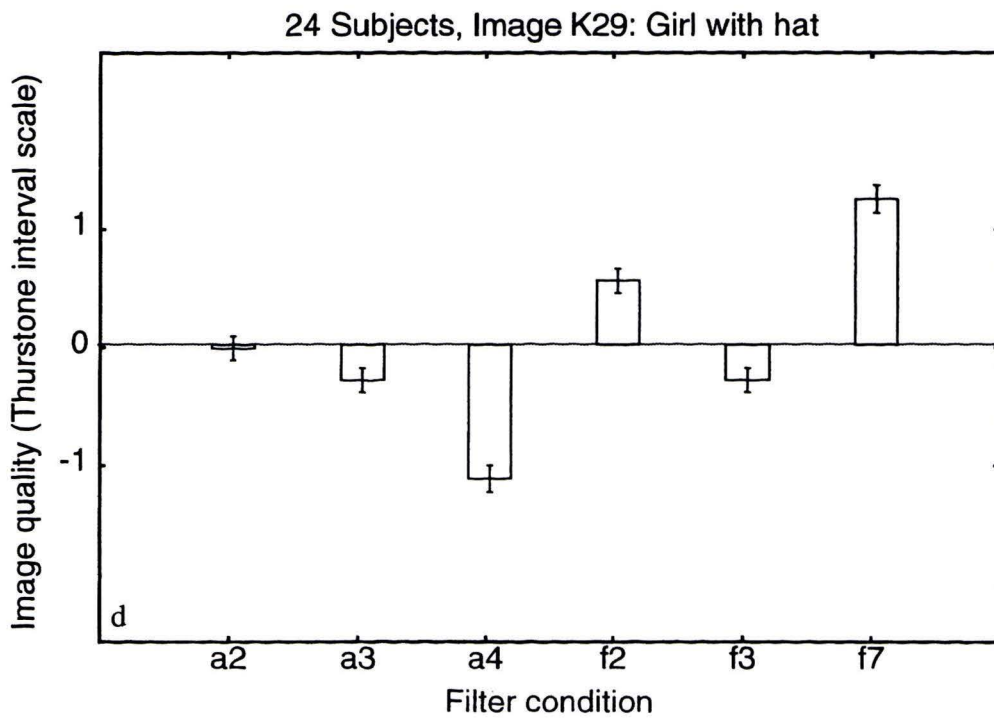
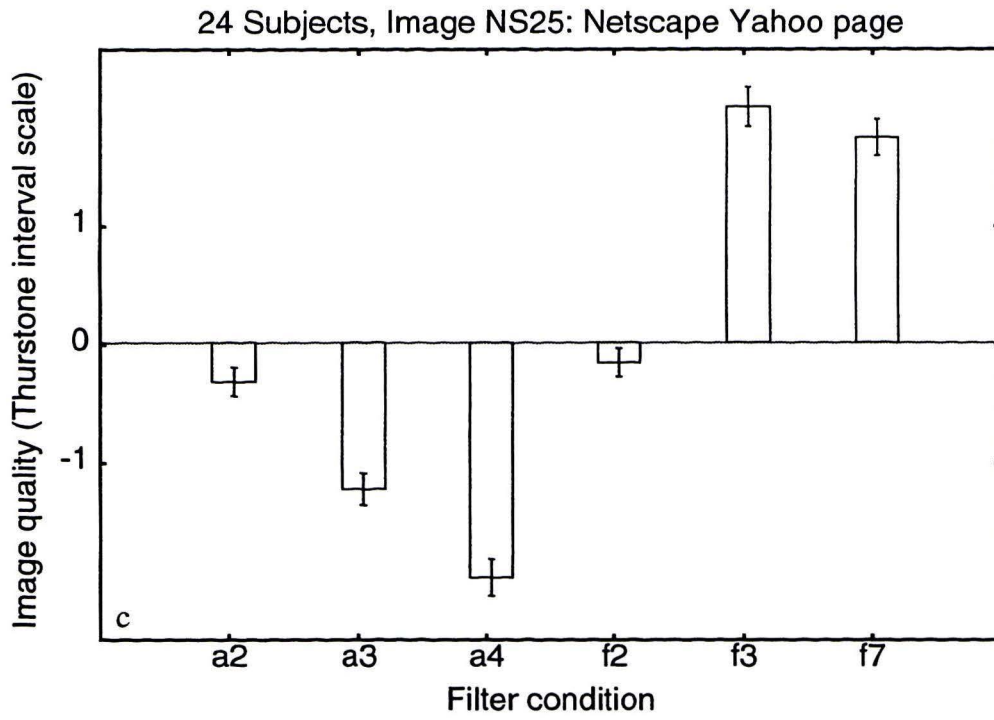


Figure 9c and 9d: Pooled quality assessment results of experiment 2 for images NS25 and K29.

kernel at positions indicated by this line detector and is therefore not very useful to prevent phi-movement. The detector needs to be extended to enable both line and edge detection in order to filter both artifacts. One may question the relevance of such an adaptive filter, as it will not only become more complex but the advantage of adaptivity becomes questionable (since both edges and lines are filtered). A preliminary test with such a more complex adaptive filter indeed showed that the difference with a fixed filter was hardly visible.

The fixed filters are always active and will therefore prevent both line-flicker and phi-movement. The different results for the portrait image is explained by the fact that the original hardly shows any line-flicker or phi-movement. Hence, for this image low-pass filtering will merely have an effect on the sharpness perceived by the subjects. The size of the filters is proportional to the amount of blur they cause in the image. This is the case for all filters except for the fixed seven-taps filter that has two negative coefficients and therefore has a deblurring property causing the image to be slightly enhanced.

5. General conclusions

This study shows that simple fixed low-pass filters are more effective than the used adaptive filters in preventing the visual disturbance artifacts line-flicker and phi-movement. The adaptive filter algorithm is not capable of detecting edges and therefore does not prevent phi-movement. In the case of an image with text and graphical information (e.g. an internet page) the best results are found for the three-taps filter, whereas in the case of a more natural image the seven-taps deblurring filter is preferred.

It is possible to modify the adaptive filter to react to both lines and edges. However, such a filter is, for all practical circumstances, equivalent to a fixed filter, so that the increased complexity of such a filter makes it unsuited.

References

- Boschman, M.C. (1996) *DIFSCAL: A program for the analysis of comparative preference scaling results*. Forthcoming manual, Institute for Perception Research (IPO), Eindhoven, The Netherlands.
- Guilford, J.P. (1954) *Psychometric methods (second edition)*. McGraw-Hill, New York.
- ISO (1992) *Ergonomic requirements for office work with visual display terminals (VDTs). Part 3: Visual display requirements*. ISO 9241-3.
- ITU (1996) *Subjective video quality assessment methods for multimedia applications*. Draft new recommendation P.910.
- Thurstone, L.L. (1927) A law of comparative judgement. *Psychological review*, 34, 273-286.
- Torgerson, W.S. (1958) *Theory and methods of scaling*. John Wiley and Sons, New York.

Appendix: Adaptive flicker-reduction filtering

In order to test the usefulness of adaptive filtering for flicker reduction, a specific algorithm had to be developed and implemented. In a recent paper (Jean-Bernard Martens, Adaptive contrast enhancement through residue-image processing, Signal Processing 44, pp 1-18, 1995) it was shown that many existing algorithms for (adaptive) filtering can be fitted into the general framework of residue-image processing. We will therefore first describe this framework and subsequently discuss the adaptations that have been made in order to use it for adaptive flicker-reduction filtering.

In residue-image processing, an output image $\hat{f}(x)$, for $x \in \mathcal{F}$, is derived from an input image $f(x)$ by combining windowed output images $f_p(x) \cdot w(x-p)$, for $p \in \mathcal{P}$, which arise through processing of windowed input images $f(x) \cdot w(x-p)$. The windowing function $w(x)$ has limited support, which means that $w(x-p)$ is zero, except in the neighbourhood of position $p \in \mathcal{P}$. The windowed images $f(x) \cdot w(x-p)$ and $f_p(x) \cdot w(x-p)$ are hence localized around position $p \in \mathcal{P}$. The processing at different window positions $p \in \mathcal{P}$ is done independently. The argument set, \mathcal{F} , is a subset of the two-dimensional Euclidean space and in our case is the non-interlaced sampling raster of the original VGA-image. The lattice \mathcal{P} could be a discrete subset of \mathcal{F} . In the flicker-reduction algorithm described below, we have chosen $\mathcal{P} = \mathcal{F}$, since we were mostly interested in studying the value of adaptive filtering for flicker reduction. Choosing \mathcal{P} to be a subset of \mathcal{F} mainly influences the computational complexity of the algorithm, which was not an issue in this exploratory study.

In the first stage of the algorithm, windowed images are derived from the non-interlaced VGA-image $f(x)$. These windowed images are subsequently decomposed as

$$w(x-p) \cdot f(x) = w(x-p) \cdot \left[\bar{f}(p) + (f(x) - \bar{f}(p)) \right],$$

where the value $\bar{f}(p)$ is fixed for a given window position $p \in \mathcal{P}$. This value can be uniquely determined by selecting it such that the weighted energy

$$e(p) = \int_{\mathcal{F}} w^2(x-p) \left[f(x) - \bar{f}(p) \right]^2 dx$$

in the residue image $f(x) - \bar{f}(p)$ is minimized. The resulting mean value

$$\bar{f}(p) = \frac{\int_{\mathcal{F}} w^2(x-p) f(x) dx}{\int_{\mathcal{F}} w^2(x-p) dx}$$

gives the minimum weighted energy. In the remainder, we will assume that the window $w(x)$ is normalized so that $\int_{\mathcal{F}} w^2(x) dx = 1$. The mean values $\bar{f}(p), p \in \mathcal{P}$ can thus be obtained by applying a filter with an impulse response $w^2(-x)$ to the

image $f(x)$ and then sampling the filtered output on the lattice \mathcal{P} (this subsampling is omitted in case $\mathcal{P} = \mathcal{F}$).

In the second stage of the algorithm, we alter the windowed images $w(x-p) \cdot f(x)$ by controlling the amplitude of the residue image, i.e., we derive processed windowed images

$$w(x-p) \cdot f_p(x) = w(x-p) \left[\bar{f}(p) + \kappa(p) \cdot (f(x) - \bar{f}(p)) \right],$$

for $p \in \mathcal{P}$. The weights $\kappa(p)$ are called the residue amplification factors. Of course, $\kappa(p) \neq 0$ only makes sense if $f(x) \neq \bar{f}(p)$, i.e., if the image $f(x)$ varies within the window $w(x-p)$. We will discuss below how the amplification factor $\kappa(p)$ should be selected in the case of line flicker reduction.

In the third stage of the algorithm, the windowed images $f_p(x) \cdot w(x-p)$, $p \in \mathcal{P}$ are combined into one output image $\hat{f}(x)$. There are many ways of constructing such an output image, but we will restrict ourselves to summations of the form

$$\hat{f}(x) = \sum_{p \in \mathcal{P}} f_p(x) w(x-p) \cdot r(x-p).$$

If all the windowed images are derived from one global input image $f(x)$, i.e., if $f_p(x) \cdot w(x-p) = f(x) \cdot w(x-p)$, for all $p \in \mathcal{P}$, then of course we expect the output to be equal to $f(x)$, for all $x \in \mathcal{F}$. This condition is satisfied by

$$r(x-p) = \frac{u(x-p)}{\sum_{q \in \mathcal{P}} w(x-q) u(x-q)},$$

provided $u(x)$ is such that

$$\sum_{q \in \mathcal{P}} w(x-q) u(x-q) \neq 0,$$

for all argument values $x \in \mathcal{F}$. An adequate choice is $u(x) = w(x)$. The resulting output image is

$$\hat{f}(x) = \sum_{p \in \mathcal{P}} f_p(x) \cdot \hat{w}(x-p),$$

with

$$\hat{w}(x) = \frac{w^2(x)}{\sum_{p \in \mathcal{P}} w^2(x-p)},$$

for $x \in \mathcal{F}$. For the case of no sub-sampling, $\mathcal{P} = \mathcal{F}$, this further simplifies to $\hat{w}(x) = w^2(x)$. This processed image $\hat{f}(x)$ is displayed in interlaced format.

The processed image can be rewritten as

$$\begin{aligned} \hat{f}(x) &= \sum_{p \in \mathcal{P}} \hat{w}(x-p) \left[\bar{f}(p) + \kappa(p) \cdot (f(x) - \bar{f}(p)) \right] \\ &= \sum_{p \in \mathcal{P}} \hat{w}(x-p) \cdot [1 - \kappa(p)] \cdot \bar{f}(p) + f(x) \cdot \sum_{p \in \mathcal{P}} \hat{w}(x-p) \cdot \kappa(p), \end{aligned}$$

for $x \in \mathcal{F}$, and hence consists of two components.

The first component is derived by interpolating the weighted mean values, $\bar{f}(p) \cdot [1 - \kappa(p)]$, $p \in \mathcal{P}$, with the aid of a filter with impulse response $\hat{w}(x)$. This component can be described as

$$\hat{f}_1(x) = \int_{\mathcal{F}} f(y) \left[\sum_{p \in \mathcal{P}} \hat{w}(x - p) \cdot [1 - \kappa(p)] \cdot w^2(y - p) \right] dy,$$

and is hence related to the input image $f(x)$ by a space-variant low-pass filter. In areas of the image where $\kappa(p) = 0$, this low-pass version of the original image is the only component present in the processed image.

The second component, $\hat{f}_2(x) = f(x) \cdot \kappa(x)$, selects specific parts of the original image by applying the global window function

$$\kappa(x) = \sum_{p \in \mathcal{P}} \hat{w}(x - p) \cdot \kappa(p),$$

for $x \in \mathcal{F}$, which is obtained by interpolating the residue amplification factors $\kappa(p)$ on the lattice \mathcal{P} . Hence, the second component only occurs in non-uniform regions of the image. In areas of the image where $\kappa(p) = 1$, this original image is the only component present in the processed image.

The overall algorithm is easily implemented with the aid of the algorithmic structure of figure 1.

For the application of flicker reduction, we only need filtering along the vertical direction. Binomial filters with impulse response

$$w^2(x) = b_N(x) = \frac{N!}{2^N (N - x)!x!},$$

for $x = 0, \dots, N$, along the vertical direction have been chosen for this purpose. The window size of this binomial filter is $N + 1$. If the residue image is suppressed at all positions, i.e., $\kappa(p) = 0$ for all $p \in \mathcal{P}$, then the adaptive algorithm will behave as a space-invariant low-pass filter with overall filter response equal to $b_{2N}(x)$ (i.e., a filter of length $2N + 1$).

For instance, in the case $N = 1$, this implies that the sampling and interpolating filters are $w^2(-x) = (0, 0.5, 0.5)$ and $\hat{w}(x) = (0.5, 0.5, 0)$, respectively. The overall space-invariant filter in case the residue image is suppressed is $b_2(x) = (0.25, 0.5, 0.25)$.

The adaptive residue-image processing algorithm assumes that we know how to derive the residue amplification factors $\kappa(p)$ from the input image. It is suggested here that this amplification factor is a function

$$\kappa(p) = \kappa[c(p)],$$

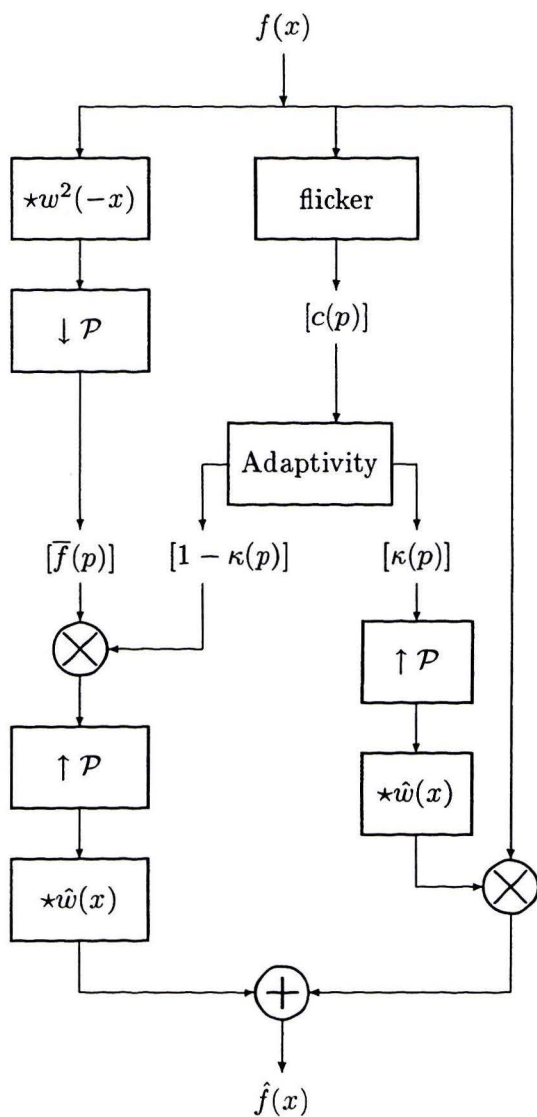


Figure 1: Structure of an adaptive residue-image processing algorithm. The boxes denoted by $\star h(x)$ indicate filtering with a filter with impulse response equal to $h(x)$, while $\downarrow \mathcal{P}$ and $\uparrow \mathcal{P}$ denote downsampling and upsampling on the lattice \mathcal{P} respectively. These down- and upsampling are not used in the current implementation. The flicker measure ‘flicker’ is detailed in Figure 2.

of some flicker measure $c(p)$ that signals the presence of line structures (i.e., positions where line flicker is expected). Such a measure can be derived from the minimum difference

$$\min(|a - b|, |a - c|),$$

where a is the current pixel value, and b and c are the pixel values on the preceding and next line, respectively. This measure will be zero in uniform regions ($a \approx b \approx c$) and edge regions ($a \approx b$ or $a \approx c$), but will react to lines. This minimum difference only gives a non-zero response at the position of the line itself, which may be too short to accomplish sufficient line-flicker reduction in the residue-image processing algorithm. A possible remedy is to extend the measure to previous and successive scan line(s) whenever a line structure is detected. This can be accomplished by filtering the minimum difference measure with a line detector filter $l_d(x)$ of length d in the vertical direction. An adequate choice is to select a uniform filter with all weights equal to one. The line-flicker criterium $c(p)$ used in the residue-image processing algorithm is hence the minimum-difference measure after filtering, as shown in Figure 2.

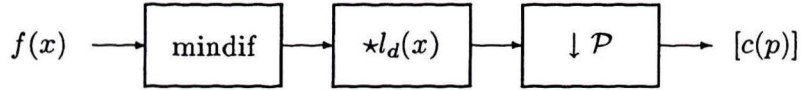


Figure 2: Algorithmic structure for deriving the line flicker measure. The line detector filter $l_d(x)$ is a uniform filter of length d along the vertical direction. The downsampling $\downarrow \mathcal{P}$ is not used in the current implementation.

In order to relate the flicker measure $c(p)$ to the residue-amplification factor, we use the following soft-threshold function

$$\kappa[c(p)] = \frac{1}{1 + [c(p)/t]^{4s}},$$

with threshold value t and slope s/t . If $c(p)$ is small ($c(p) < t [1 - 1/(2s)]$), i.e., in the absence of line flicker, $\kappa(p) \approx 1$ and the original image is output. If $c(p)$ is large ($c(p) > t [1 + 1/(2s)]$), i.e., in the presence of line flicker, $\kappa(p) \approx 0$ and the image is low-pass filtered with $w^2(x) \star w^2(-x) = b_{2N}(x)$.